Supplementary Material for:

CpG methylation differences between neurons and glia are highly conserved from mouse to human

Noah J. Kessler[1], Timothy Van Baak[1], Maria Baker[1], Eleonora Laritsky[1], Cristian Coarfa[2], Robert A. Waterland[1,3,*]

[1]Department of Pediatrics, Baylor College of Medicine, USDA/ARS Children's Nutrition Research Center

[2]Department of Molecular & Cell Biology, Baylor College of Medicine

[3]Department of Molecular & Human Genetics, Baylor College of Medicine, USDA/ARS Children's Nutrition Research Center, 1100 Bates St., Ste. 5080, Houston, TX 77030, USA

Contents

Link to UCSC Genome Browser including our representation of Lister & Mukamel et al.'s Bisulfite-seq data on Neuron vs. Glia methylation differences in mouse cortex:

http://genome.ucsc.edu/cgi-bin/hgTracks?hgS_doOtherUser=submit&hgS_otherUserName=noah.kessler&hgS_otherUserSessionName=Lister%2DMukamel%20mm9%20Pub

Figure S1. Examples of genomic regions showing neuron vs. glia methylation differences.

Figure S2. CpG density distributions among genes classified as differentially methylated either by Lister & Mukamel et al or by our analysis.

Figure S3. $NeuN^+$ and $NeuN^-$ nuclei were sorted well by fluorescence-activating sorting.

Figure S4. Size and CpG content of neuron vs. glia DMRs identified by the MOABS analysis.

Figure S5. Distribution of credible differences in proportional methylation [abs($NeuN^+$ - $NeuN^-$)] identified by the MOABS analysis.

Figure S6. Comparison of genes identified as showing neuron vs. glia differential methylation by MOABS vs. our analysis.

Figure S7. Comparison of genes identified as showing neuron vs. glia differences in methylation in human cortex by Guintivano et al. vs. in our analysis of the Lister & Mukamel et al human data.

Figure S8. Conservation of gene-specific neuron vs. glia methylation differences between mouse and human cortex is associated with sequence-level conservation

Figure S9. Pyrosequencing standards for each assay used for validation confirm the accuracy of the assays.

(Supplementary Tables are included separately as an Excel file.)

Figure S1 (1st of 3 pages)

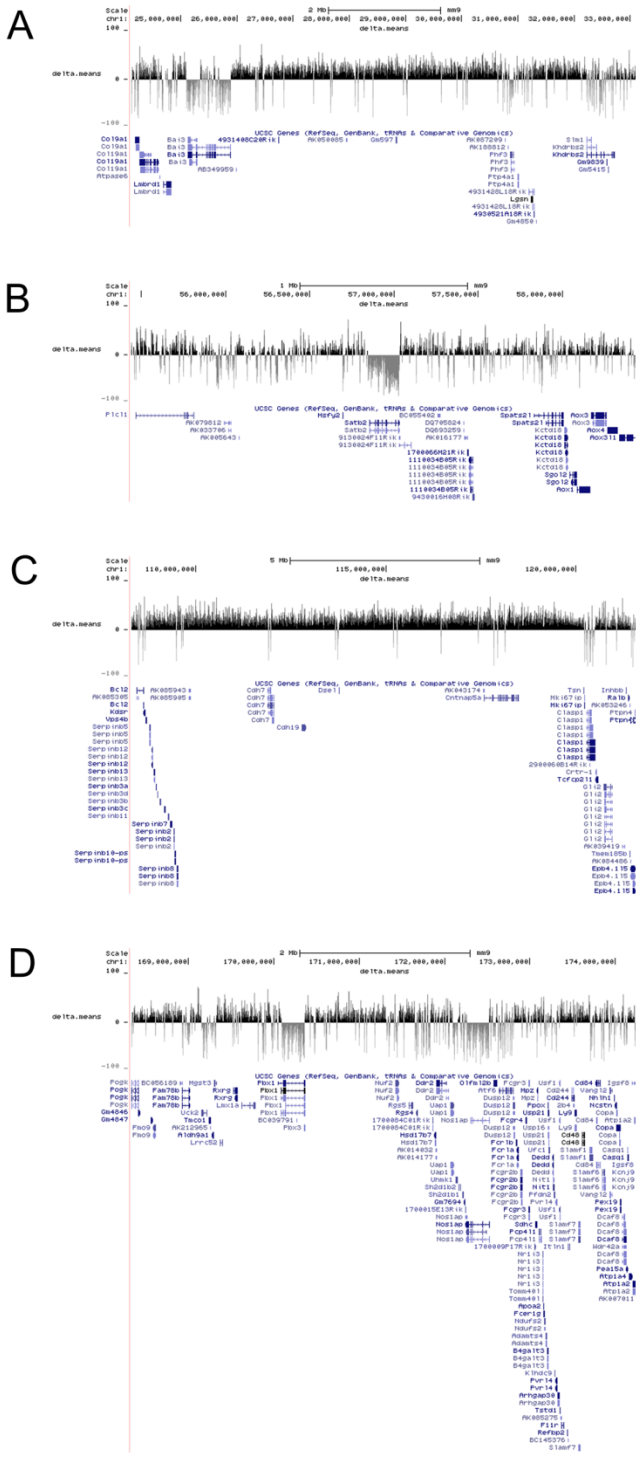

Figure S1 (cont.)

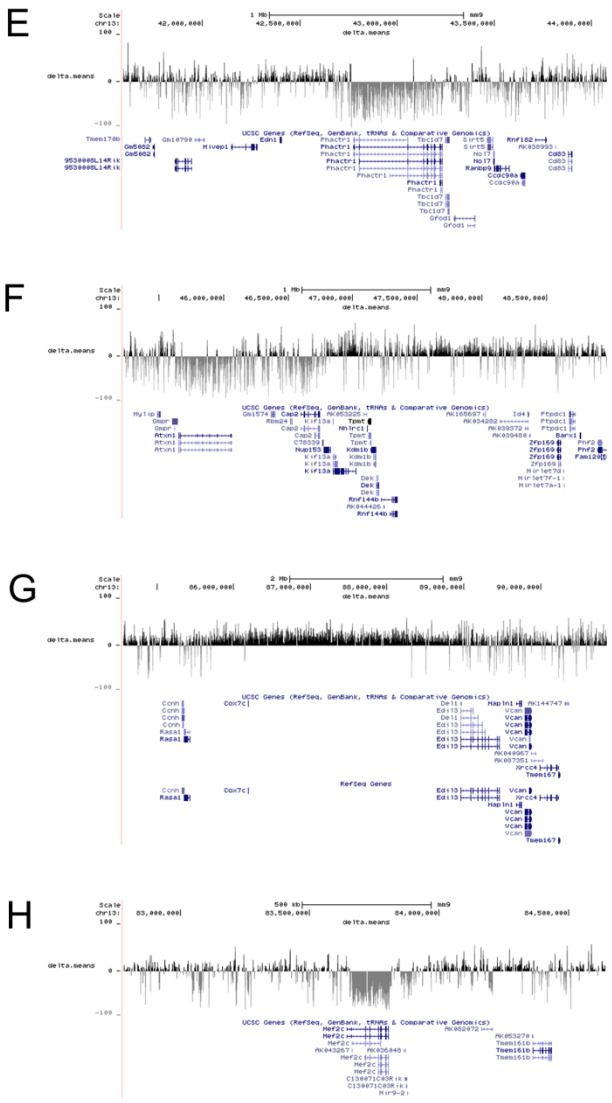

Figure S1 (cont.)

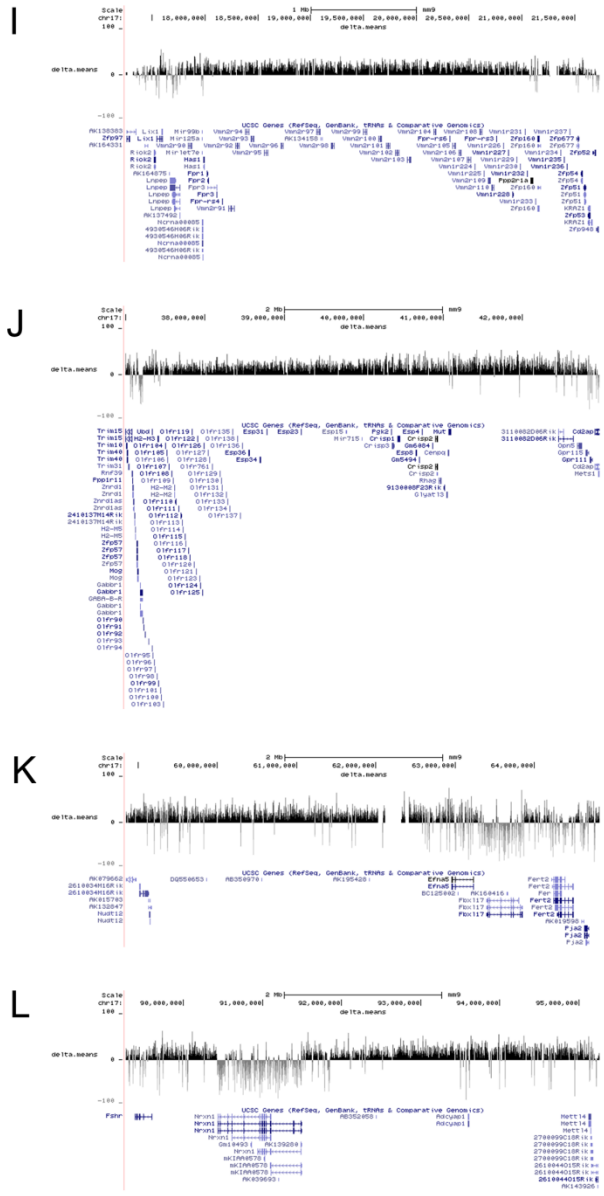

Figure S1. Examples of genomic regions showing neuron vs. glia methylation differences. Plotted are mean deltas (Average NeuN+ % methylation) – (Average NeuN- % methylation) for all informative 200bp bins.

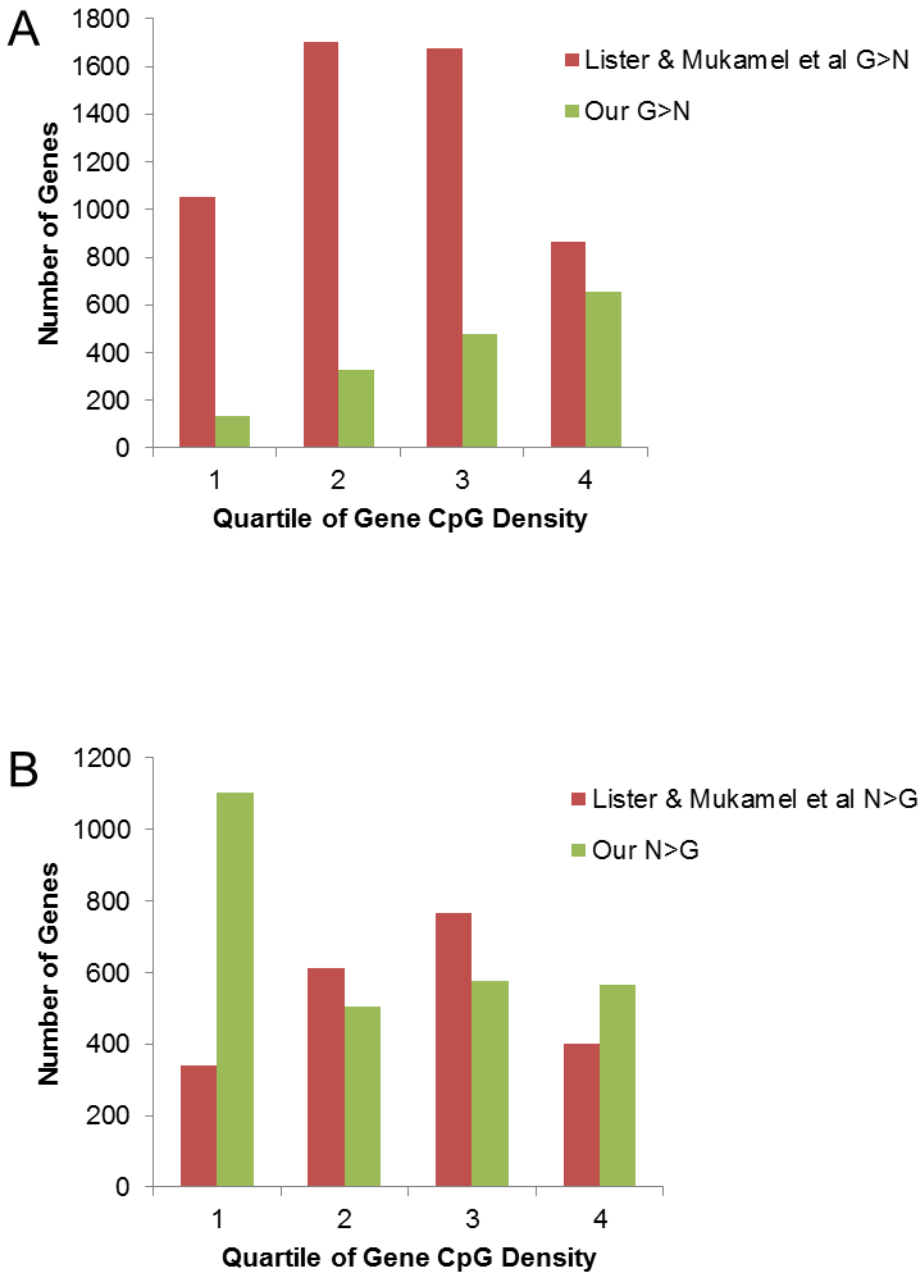

Figure S2. CpG density distributions among genes classified as differentially methylated either by Lister & Mukamel *et al*. or by our analysis. Among genes classified as either G>N (**A**) or N>G (**B**), the greatest discrepancies between the two analyses occur at genes with lower CpG density.

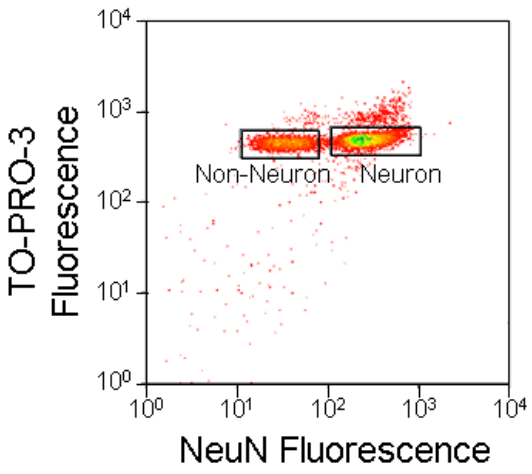

Figure S3. NeuN$^+$ and NeuN$^-$ nuclei were sorted well by fluorescence-activated sorting. The two rectangles represent the gates of NeuN and TO-PRO-3 levels used for sorting nuclei.

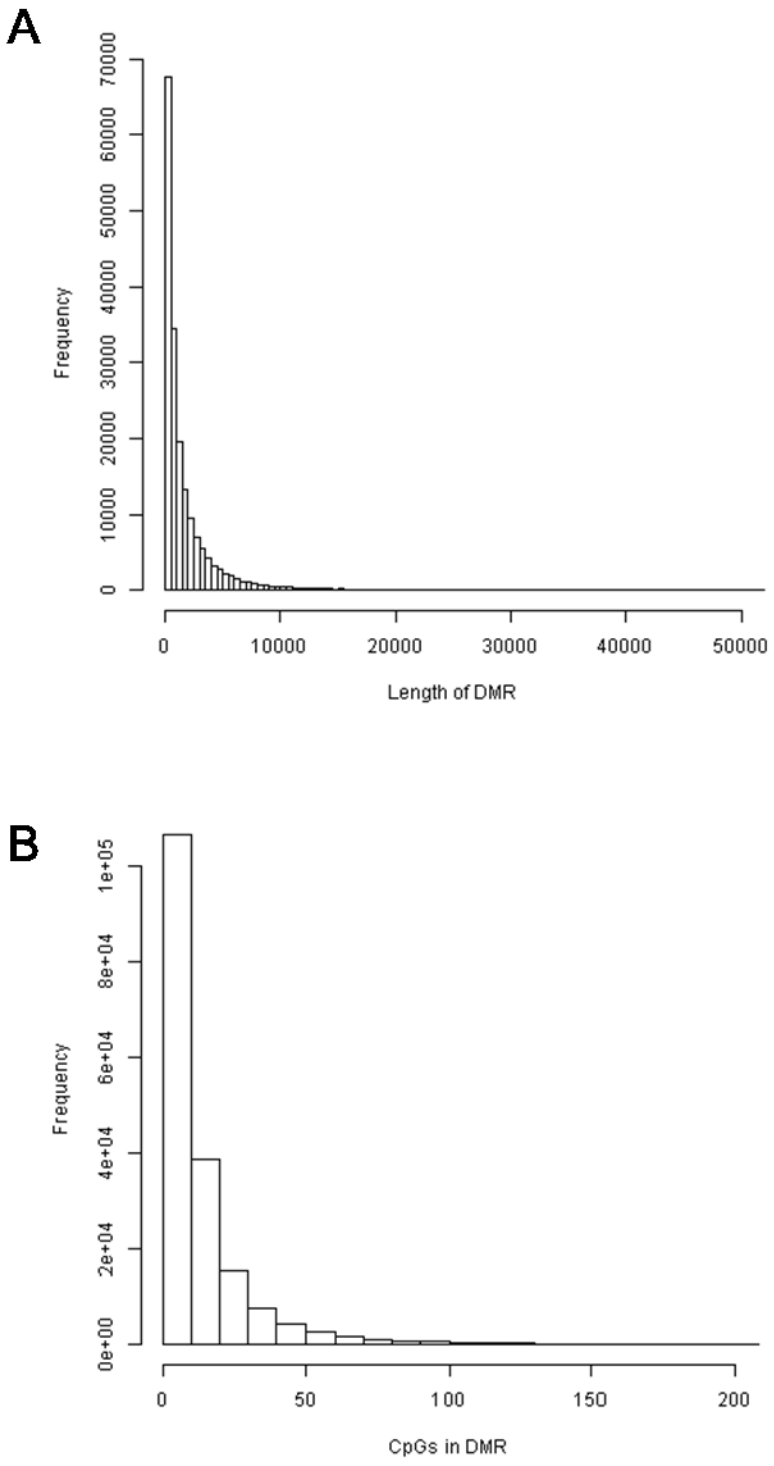

Figure S4. Size and CpG content of neuron vs. glia DMRs identified by the MOABS analysis. (**A**) Distribution of DMR size. Most DMRs are less than 20kb long. (**B**) Distribution of CpG content per DMR. Most DMRs encompass fewer than 150 CpG sites.

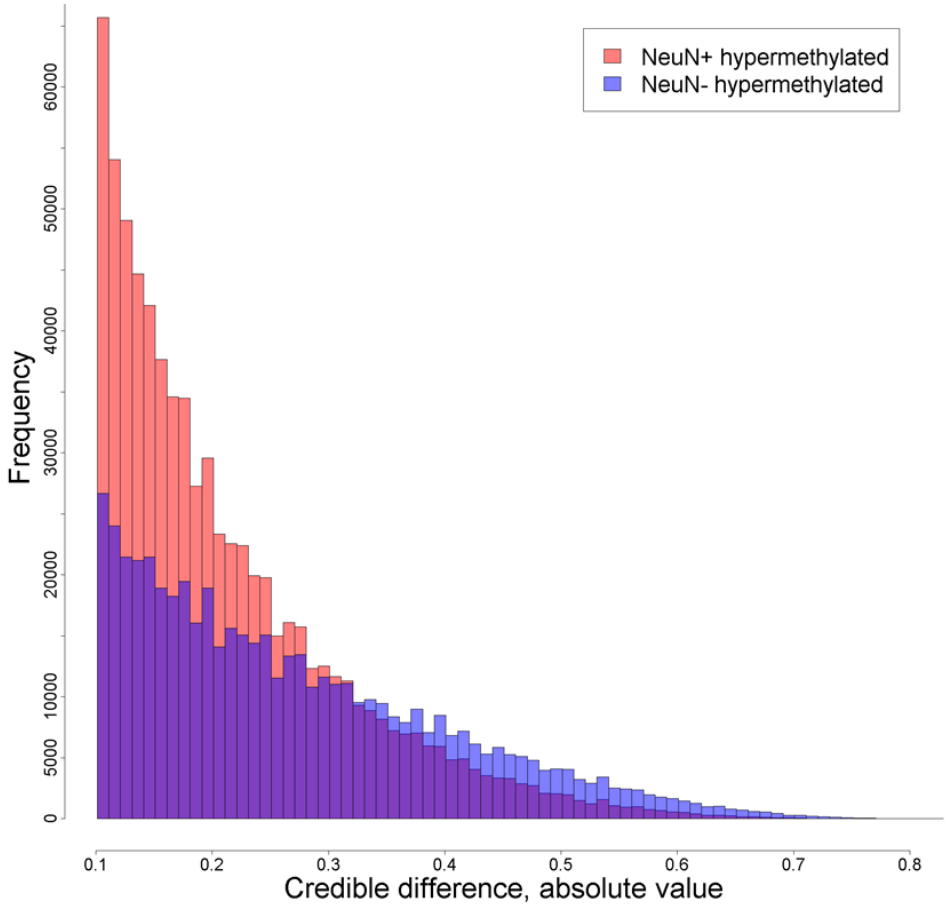

Figure S5. Distribution of credible differences in proportional methylation [abs($NeuN^+$ - $NeuN^-$)] identified by the MOABS analysis. Although more DMRs indicated relative hypermethylation in neurons relative to glia ($NeuN^+$ hypermethylated, red) DMRs with relative hypermethylation in glia relative to neurons ($NeuN^-$ hypermethylated, blue) tended to reflect greater cell-type differences in methylation.

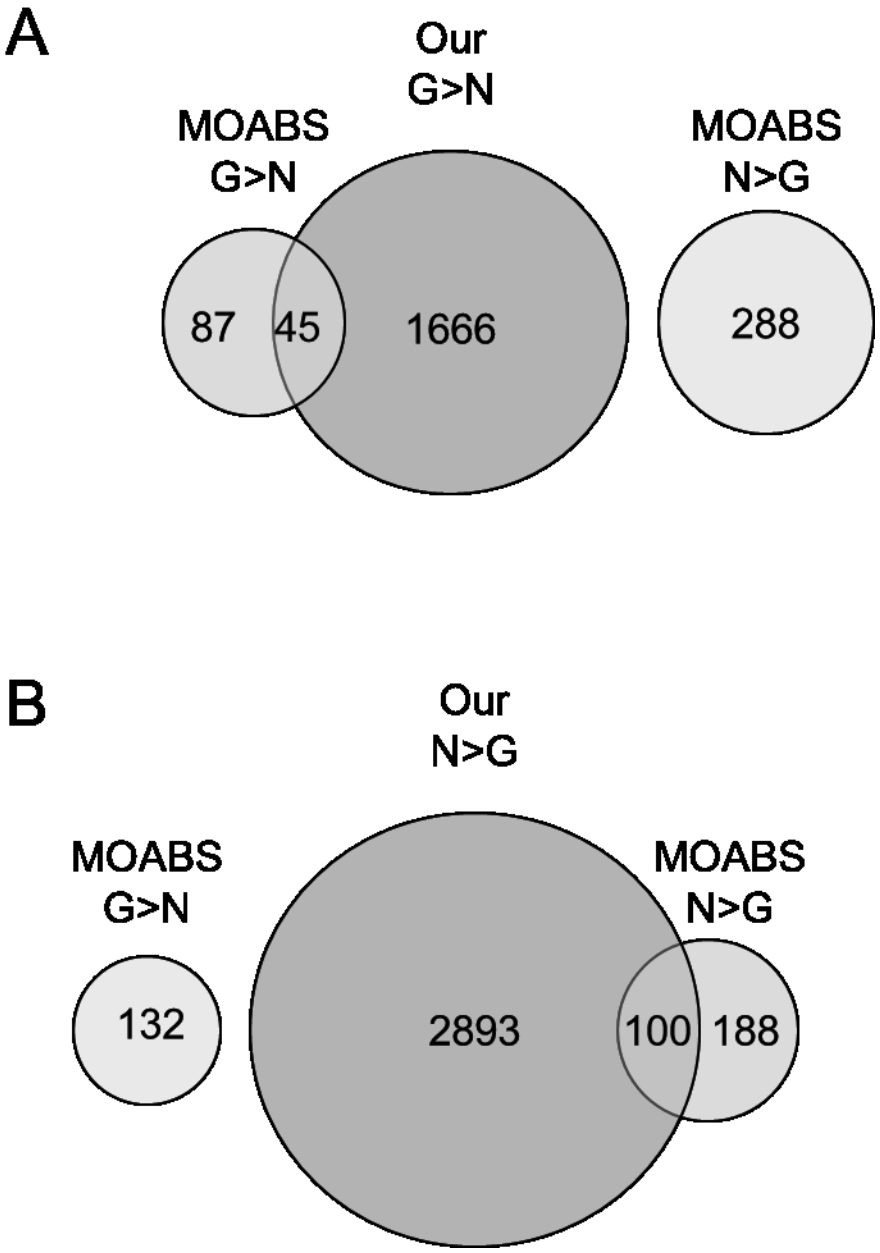

Figure S6. Comparison of genes identified as showing neuron vs. glia differential methylation by MOABS vs. our analysis. (A) Over 1/3 of the 132 genes identified as G>N by MOABS were likewise classified in our analysis. None of the 288 genes identified by MOABS as N>G were classified oppositely by our analysis. (B) Likewise, over 1/3 of the 288 genes identified as N>G by MOABS were likewise classified in our analysis. None of the 132 genes identified by MOABS as G>N were classified oppositely by our analysis.

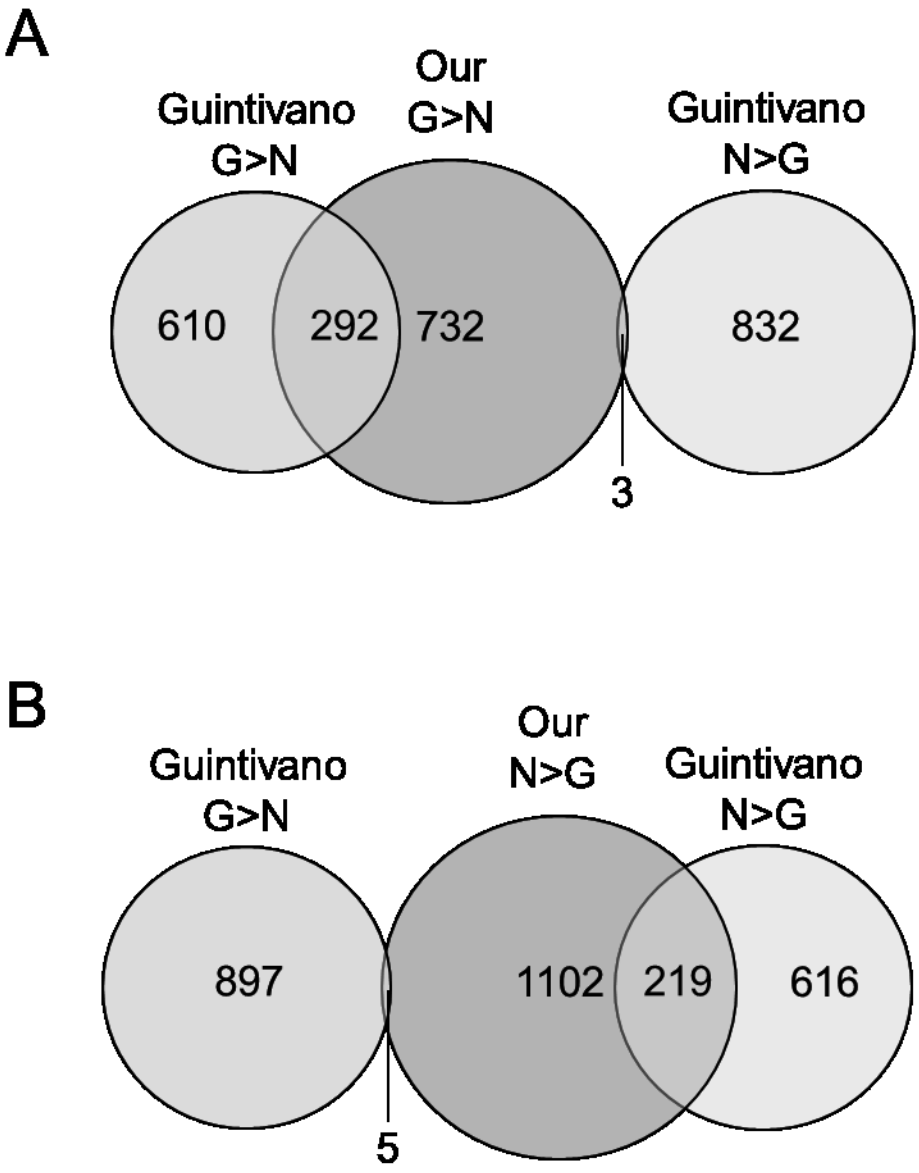

Figure S7. Comparison of genes identified as showing neuron vs. glia differences in methylation in human cortex by Guintivano et al. vs. in our analysis of the Lister & Mukamel et al human data. (A) Nearly 1/3 of the 902 genes identified as G>N in the data of Guintivano et al. were likewise classified in our analysis of the data of Lister & Mukamel et al. Only 3 genes identified by Guintivano et al. as N>G were classified oppositely by our analysis. (B) About 1/4 of the 835 genes identified as N>G in the data of Guintivano et al. were likewise classified in our analysis. Only 5 of the 902 genes identified by Guintivano et al. as G>N were classified oppositely by our analysis.

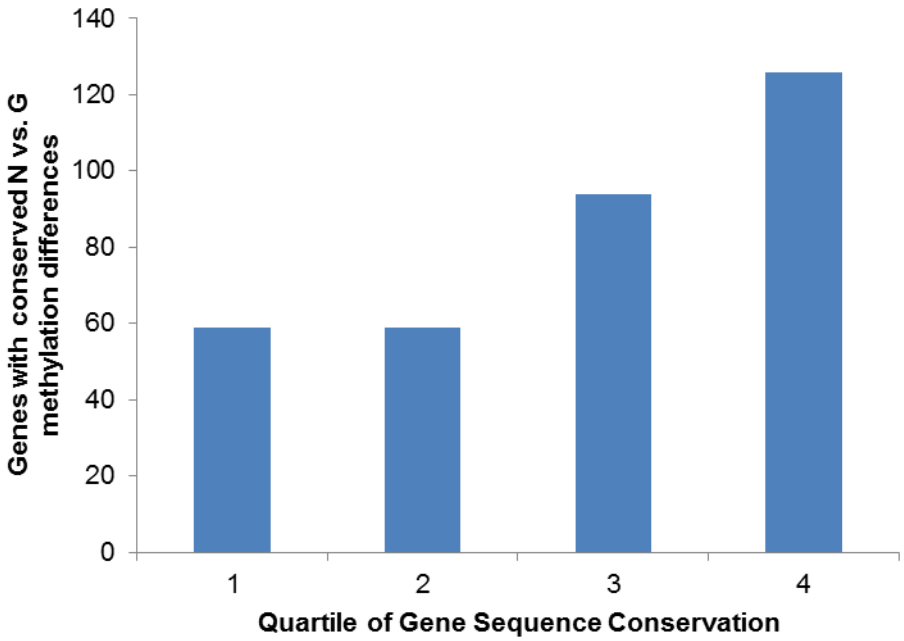

Figure S8. Conservation of gene-specific neuron vs. glia methylation differences between mouse and human cortex is associated with sequence-level conservation ($P=5.0 \times 10^{-8}$, chi-squared test).

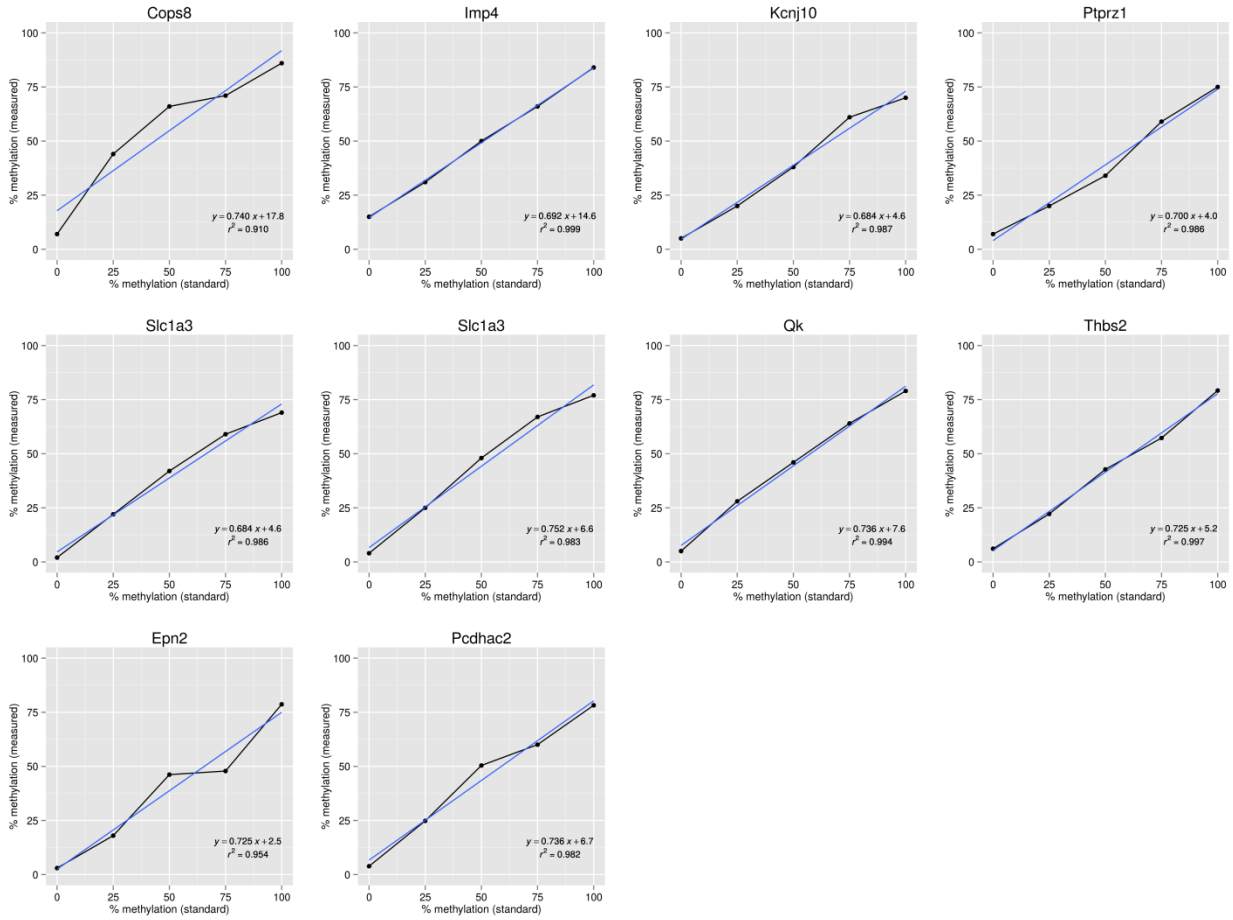

Figure S9. Pyrosequencing standards for each assay used for validation confirm the accuracy of the assays. For each of the nine genes in Figs. 3-4, standards were run on the corresponding pyrosequencing assays. The slopes, intercepts, and R^2 of each plot indicate that the bisulfite pyrosequencing results of these genes can be used with confidence. Note that there are two standards plots for *Slc1a3* as two separate assays were used for this gene.